

Characteristics of Repetitive Positioning Control of a Linear Pulse Servo Motor

Masayasu Yamamoto and Kouki Matsuse

Department of Electrical Engineering, Meiji University
1-1-1, Higashi-mita, Tama-ku, Kawasaki 214-8571, JAPAN
Phone: +81-044-934-7293, Fax: +81-044-934-7293

Abstract - This study aims to realize high precision repetitive positioning control of the linear servo motor. The authors have previously improved the repeatability positioning precision by employing a two-degree-of-freedom PID controller in the positioning control system and by upgrading the drive system. The present study focuses on variable distance repetitive positioning control, rather than equal distance positioning, and investigates the repeatability positioning precision.

1. INTRODUCTION

Two conditions must generally be met for the positioning control system of a linear servo motor drive: high response and the suppression of external disturbances which act to lower the positioning accuracy. To this end, the use of a two-degree-of-freedom controller, which meets these conditions independently, has been proposed for positioning control [1][2]. Yet, to achieve a highly precise repetitive positioning control, it becomes necessary to deal with positioning errors that cannot be controlled by the positioning controller alone. Here, if one notices that positioning consists of periodic repetitive motion, it becomes clear that the use of a repetitive controller can improve the repeatability positioning precision [3][4]. The present study examines the repeatability positioning precision of variable distance repetitive positioning control, rather than the conventional equal distance positioning.

This paper first examines two different drive systems and their effects on repeatability positioning precision, then discusses the repetitive controller and its features.

2. LINEAR PULSE MOTOR AND DRIVE SYSTEM

2.1 Motor Construction

Figure 1 shows the basic construction of the tested 3-phase 12-pole PM type linear pulse motor. The motor mover is mounted with a Magnetic Resistance(MR) sensor unit, which detects the motor position and 3-phase pole position signals. This makes it possible to drive the Linear Pulse Motor as a servo motor and reduces the risk of "step out". Table 1 lists the main specifications of the motor.

2.2 Drive System

Figure 2 shows the circuit configuration of the linear pulse servo motor drive system. The encoder signals and 3-phase pole position signals are detected by the MR sensor unit. The current reference I_m^* is calculated with a digital computer PC9801. The 3-phase ac current references, denoted by i_u^* , i_v^* and i_w^* , are obtained by multiplying I_m^* with the 3-phase sinusoidal pole position signals.

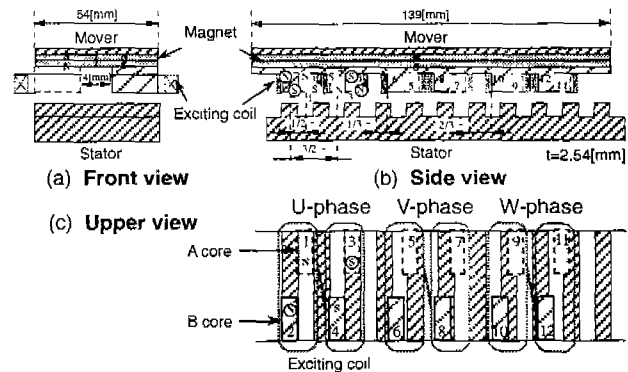


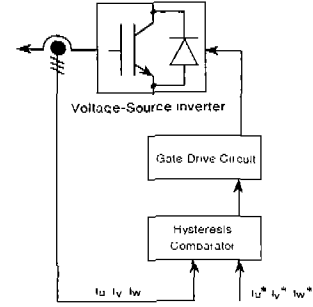
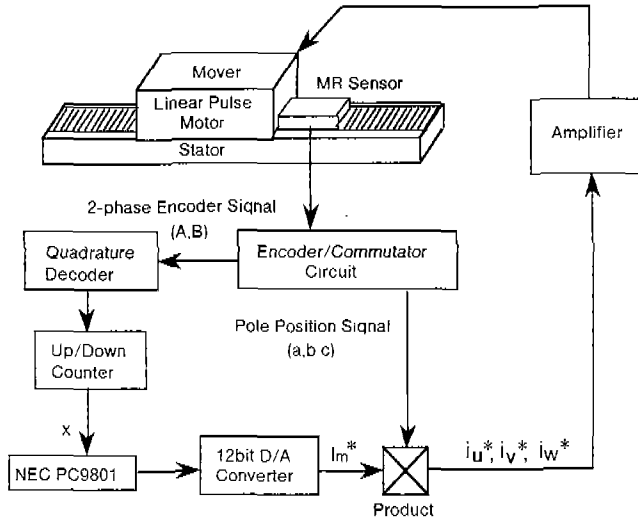
Figure 1. Basic construction of the PM type linear pulse motor.

Table 1. Main specifications of the tested the linear pulse motor.

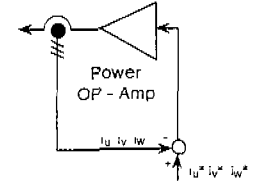
Windings	3-phase star connection
Tooth pitch	2.54[mm]
No.of teeth/pole	5
No.of turns/phase	50
Rated current	2.1[A]

Table 2. Main features of the Dual modes IPM.

High output	50[V] 25[A]
Over-current self-limited around	25[A]
External current shutdown control	
Voltage gain	100



(a) IGBT inverter



(b) Dual mode IPM inverter

Figure 2. Drive system for the linear pulse motor.

This study employs a drive system with an IGBT-composed PWM-inverter and one with an inverter composed of a High-power LINEAR/PWM Dual mode Intelligent Power Module (IPM) to examine the effect that different of the drive system construction have on the repeatability positioning precision of the Linear Pulse Motor [5]. The PWM control drive system is made to follow the current by PWM control voltage-source inverter, as shown in Fig 2(a). Meanwhile, the Dual mode IPM is essentially a linear amplifier, so its drive system follows current by voltage amplification in response to the difference between the command current reference and actual current, as shown in Fig 2(b). The main features of the Dual mode IPM are listed in Table 2.

3. TWO-DEGREE-OF-FREEDOM CONTROLLER

3.1 Basic Structure

Figure 3 shows a block diagram of the Two-Degree-of-Freedom position control system. The elements of the controller C_1 and C_2 are given by (1) and (2), respectively.

$$C_1(s) = (1 - \alpha)K_p + K_i / s + (1 - \beta)K_d s \quad (1)$$

$$C_2(s) = \alpha K_p + \beta K_d s \quad (2)$$

The differential equation of the linear pulse motor is given by (3), which can be simplified as (4).

$$M_n \ddot{x} + 2M_n \gamma \dot{x} = k_n I_m \quad (3)$$

where M_n : mover mass, γ : damping coefficient, k_n : thrust constant.

$$M_n \ddot{x} = k_n I_m \quad (4)$$

Here the influence of viscosity is included as part of the disturbances.

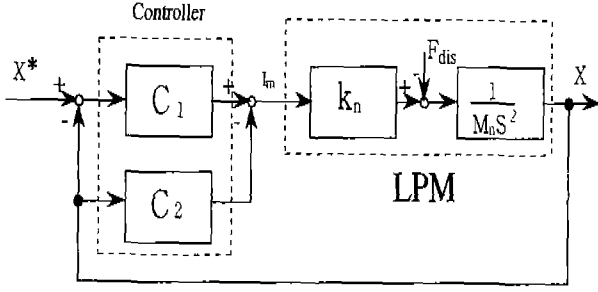


Figure 3. Block diagram of a positioning-control system using the Two-Degree-of-Freedom controller.

3.2 Controller Design

The following specifications were set for the controllers design.

<1>The closed-loop transfer function x/x^* G_{cp} can be expressed by a first-order lag element with a cut-off frequency.

<2> The complementary sensitivity function T , which indicates the characteristic in response to noise, was approximately fixed the frequency region.

We discuss these in more detail below.

<1> It is important in positioning-control systems to suppress overshoots and transient vibrations. The control design thus employs a closed-loop transfer function (x/x^*) based on the command reference.

The closed-loop transfer function (x/x^*) with command reference G_{cp} and the closed-loop transfer function (x/F_{dis}) with disturbance G_{cd} are respectively written as (5) and (6).

$$G_{cp}(s) = K \cdot \frac{(1-\beta)s^2 + (1-\alpha)q_1s + q_1q_2}{s^3 + Ks^2 + Kq_1s + Kq_1q_2} \quad (5)$$

$$G_{cd}(s) = \frac{1}{M_n} \frac{s}{s^3 + Ks^2 + Kq_1s + Kq_1q_2} \quad (6)$$

where $K = k_n K_p / M_n$, $q_1 = K_p / K_D$, $q_2 = K_I / K_p$

Here, it is desirable that the command reference response has no overshoot and that the cut-off frequency can be set freely. So we assume that G_{cp} can be expressed by a first-order lag element with a cut-off frequency ω_b as follows (7).

$$G_{cp}(s) = \frac{\omega_b}{s + \omega_b} \cdot \frac{(s + \omega')^2}{(s + \omega')^2} \quad (7)$$

$$G_{cp}(s) = \frac{\omega_b}{s + \omega_b} \quad (11)$$

Table 3. Parameters of Two-Degree-of-Freedom PID controller.

$$\begin{aligned} K_p &= \varepsilon(\varepsilon + 2)\omega_b^2 M_n / k_n \\ K_I &= \varepsilon^2 \omega_b^3 M_n / k_n \\ K_D &= (2\varepsilon + 1)\omega_b M_n / k_n \\ \alpha &= \varepsilon / (\varepsilon + 2) \\ \beta &= 2\varepsilon / (2\varepsilon + 1) \end{aligned}$$

Table4. Parameters for setting up the controller.

Parameter	Symbol	Value
Mover mass	M_n	6.7[kg]
Thrust constant	k_n	28[N/A]
Cutoff frequency	ω_b	40[rad/s]
The constant	K	200

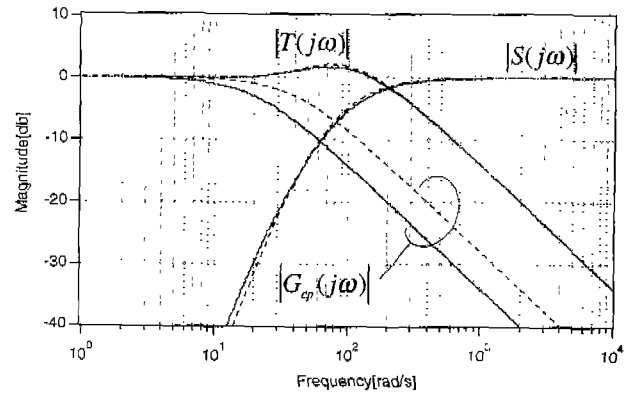


Figure 4. Calculations of the frequency characteristics (Thick line: $\omega_b = 20$ [rad/s], Broken line: $\omega_b = 40$ [rad/s] when $K=200$).

Thus, the conditional equations (8), (9) and (10) are calculated.

$$(1-\beta)K - q_2 = (1-\alpha) \left(K - \frac{1-\alpha}{1-\beta} q_1 \right) \quad (8)$$

$$(1-\beta)K = K - \frac{1-\alpha}{1-\beta} q_1 = \omega_b \quad (9)$$

$$(1-\alpha)^2 q_1 - 4q_2(1-\beta) = 0 \quad (10)$$

When the conditional equations are met, the closed-loop transfer functions G_{cp} and G_{cd} can be rewritten as (11) and (12) respectively.

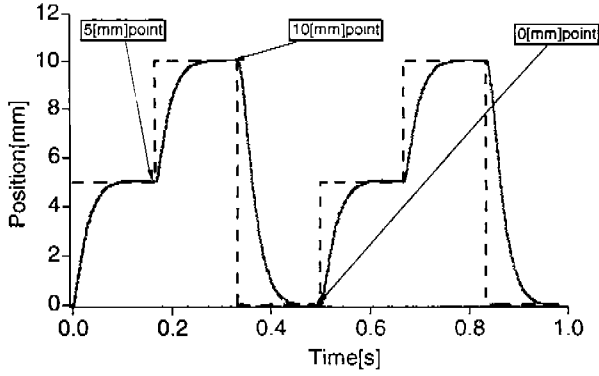


Figure 5. Experimental result of repetitive positioning-control response.

$$G_{cd}(s) = \frac{1}{M_n} \cdot \frac{s}{(s + \omega_b)(s + \varepsilon\omega_b)^2} \quad (12)$$

where $\varepsilon = 2\alpha/(1-\alpha)$, $\varepsilon \geq 1$

We can see that the parameter ω_b is determined from the response frequency and that ε is determined so as to suppress the disturbances effectively. The rearranged parameters of the Two-Degree-of-Freedom controller are now calculated as follows (13).

$$\left. \begin{aligned} \alpha &= \frac{\varepsilon}{\varepsilon+2} & \beta &= \frac{2\varepsilon}{2\varepsilon+1} & K &= (2\varepsilon+1)\omega_b \\ q_1 &= \frac{\varepsilon(\varepsilon+2)}{2\varepsilon+1}\omega_b & q_2 &= \frac{\varepsilon}{\varepsilon+2}\omega_b \end{aligned} \right\} \quad (13)$$

<2> The frequency characteristics of the positioning-control system are considered when parameters ω_b and ε are varied. It is generally important to reduce the effect of noise in the high frequency region. In our method, the parameters ω_b and ε are adjusted after the complementary sensitivity function T , which indicates noise characteristics, has been approximately fixed in a frequency region with low noise effects. The complementary sensitivity function T and the sensitivity function S are written as (14) and (15) respectively.

$$T(s) = K \cdot \frac{s^2 + q_1s + q_1q_2}{s^3 + Ks^2 + Kq_1s + Kq_1q_2} \quad (14)$$

$$S(s) = \frac{s}{s^3 + Ks^2 + Kq_1s + Kq_1q_2} \quad (15)$$

As a method to approximately fix the complementary sensitivity function T the parameter K is kept constant.

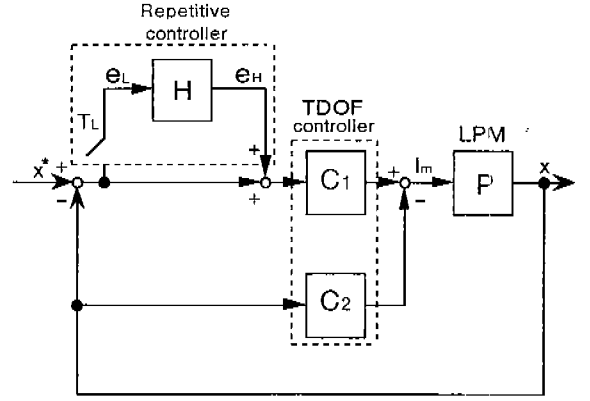


Figure 6. Block diagram of the repetitive positioning-control system with repetitive controller.

Figure 4 shows calculations of the frequency characteristics of G_p , T and S . Note that T and S are approximately fixed in the frequency region even when the cut-off frequency ω_b is varied. The parameter ε is determined the given K and ω_b , by the following equation,

$$\varepsilon = \frac{1}{2} \left(\frac{K}{\omega_b} - 1 \right) \quad (16)$$

Substituting ε into Eq.(13), all parameters of the Two-Degree-of-Freedom PID controller are calculated. Table 3 shows the Two-Degree-of-Freedom controller parameters by the proposed method.

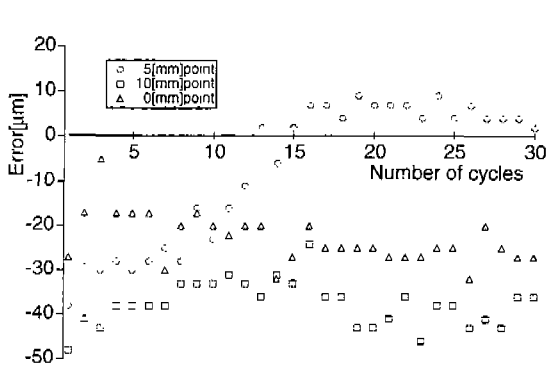
4. EXPERIMENTS

4.1 Experimental Setup

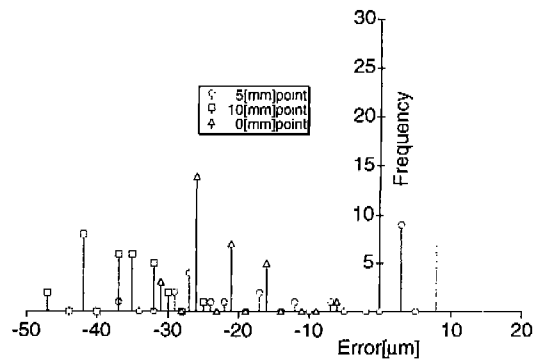
The digital control system is composed of an NEC PC9801 desktop computer. The sampling period is $500[\mu m]$, the encoder resolution is $2.48[\mu m]$ and the current limitation is $5[A]$. The parameters for setting up the controller are listed in Table 4.

4.2 Repetitive Positioning Control

Figure 5 shows the experimental result of the repetitive positioning-control response. The command reference has a frequency of $2[Hz]$. The motor is operated for thirty cycles as shown in Fig.5, and the positioning errors at the $5[mm]$, $10[mm]$ and $0[mm]$ points are detected for each cycle. These positioning errors are shown on the left side of Fig.7. The right side of Fig.7 shows the error distribution, where random

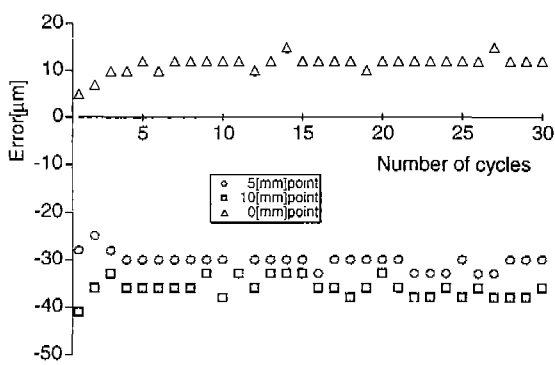


(1) Error-Number of cycles characteristic

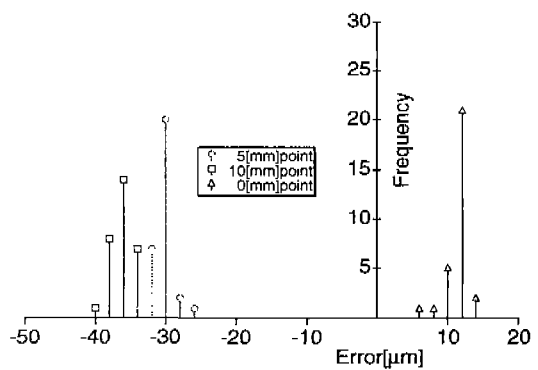


(2) Frequency-Error characteristic

(a) by PWM control drive system

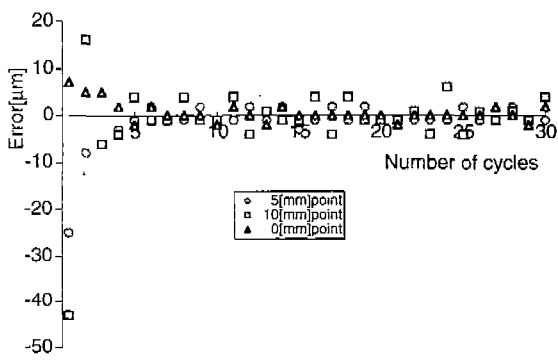


(1) Error-Number of cycles characteristic

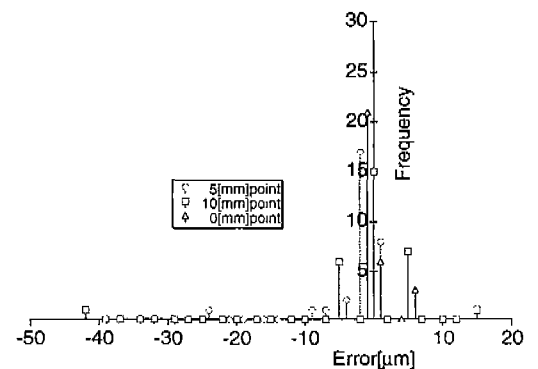


(2) Frequency-Error characteristic

(b) by the Dual mode IPM drive system.



(1) Error-Number of cycles characteristic



(2) Frequency-Error characteristic

(c) Sinusoidal drive by the Dual mode IPM drive system with a repetitive controller.

Figure 7. Experimental results of error distribution

and systematic errors are easily recognized.

Figure 7(a), (b) show respectively the experimental results of using the PWM control drive system and the Dual mode IPM control drive system. The Dual mode IPM control drive system drives the motor sinusoidally. We see that the Dual mode IPM control drive system is better suited for suppressing random errors compared to the PWM control drive system, for the reason that sinusoidal drive lowers the effects of harmonic components. The systematic error however is not suppressed, as seen in Fig.7(b). Therefore, a repetitive controller is added on to the conventional positioning-control system in order to suppress the systematic error.

4.3 Repetitive Controller

Figure 6 shows a block diagram of the repetitive positioning-control systems for the linear pulse motor with repetitive controller. The sampling interval T_L is the period of the command reference. The repetitive controller can be easily formed using a digital computer as follows (17).

$$e_n[n+1] = \sum_k^n e_r[k] \quad (17)$$

where $e_r[n+1]$: a compensated value on $(n+1)$ th cycle

$e_r[n]$: a positioning error on (n) th cycle

It can be seen that the repetitive controller is functions to counteract the systematic error in the command reference.

Figure 7(c) shows experimental results using the Dual mode IPM control drive system with the repetitive controller. We see that the systematic error is suppressed in Fig.7(c) in comparison to Fig.7(b). Note, however that a positioning error exists in the first cycle, when the repetitive controller is still not operating.

5. CONCLUSION

This study examined the repeatability positioning precision when different command references are given.

Experimental results clearly show that the Dual mode IPM control drive system effectively suppresses random errors as compared to the PWM control drive system, while the systematic error can be suppressed with a repetitive controller.

Our results indicated that the proposed method should give satisfactory results even with multiple positioning cycles

provided that the motion repetitive.

6. ACKNOWLEDGMENTS

The authors wish to thank Nihon Inter Electronics Corp, who kindly provided us with a Dual mode IPM unit, and also its staff members K. Saitou, Y. Jinriki and M. Mitome of for many fruitful discussions.

7. REFERENCES

- [1] M. Sugiura, S. Yamamoto, K. Matsuse, "Performance Evaluation of a Linear Pulse Servo Motor Position Control System with Two-Degree-of-Freedom Controller", Proc. of LDIA'95, pp.283-286, 1995.
- [2] M. Sugiura, S. Yamamoto, J. Sawaki, K. Matsuse, "The Basic Characteristics of Two-Degree-of-Freedom PID Position Controller using a Simple Design Method for Linear Servo Motor Drives", Proc. of AMC'96-MIE, Vol. 1, pp. 59-64, 1996.
- [3] J. Sawaki, S. Yamamoto, K. Matsuse, "Improved Performance of a Linear Pulse Motor with Repetitive Positioning Control", Proc. of '96 KACC, pp. 389-392, 1996.
- [4] M. Nakano, T. Inoue, Y. Yamamoto, S. Hara, "Repetitive Control", The Society of Instrument and Control Engineers Iobrary, pp.82, book JAPAN. 1989.
- [5] M. Mitome, N. Tokuda, K. Matsuse, "A NEW HIGH-power LINEAR/PWM Dual modes IPM", Proc. of IPEC'95, Vol. 2, pp. 1111-1115, 1995.